

77135

Poikilitic Impact-melt Breccia

337.4 grams

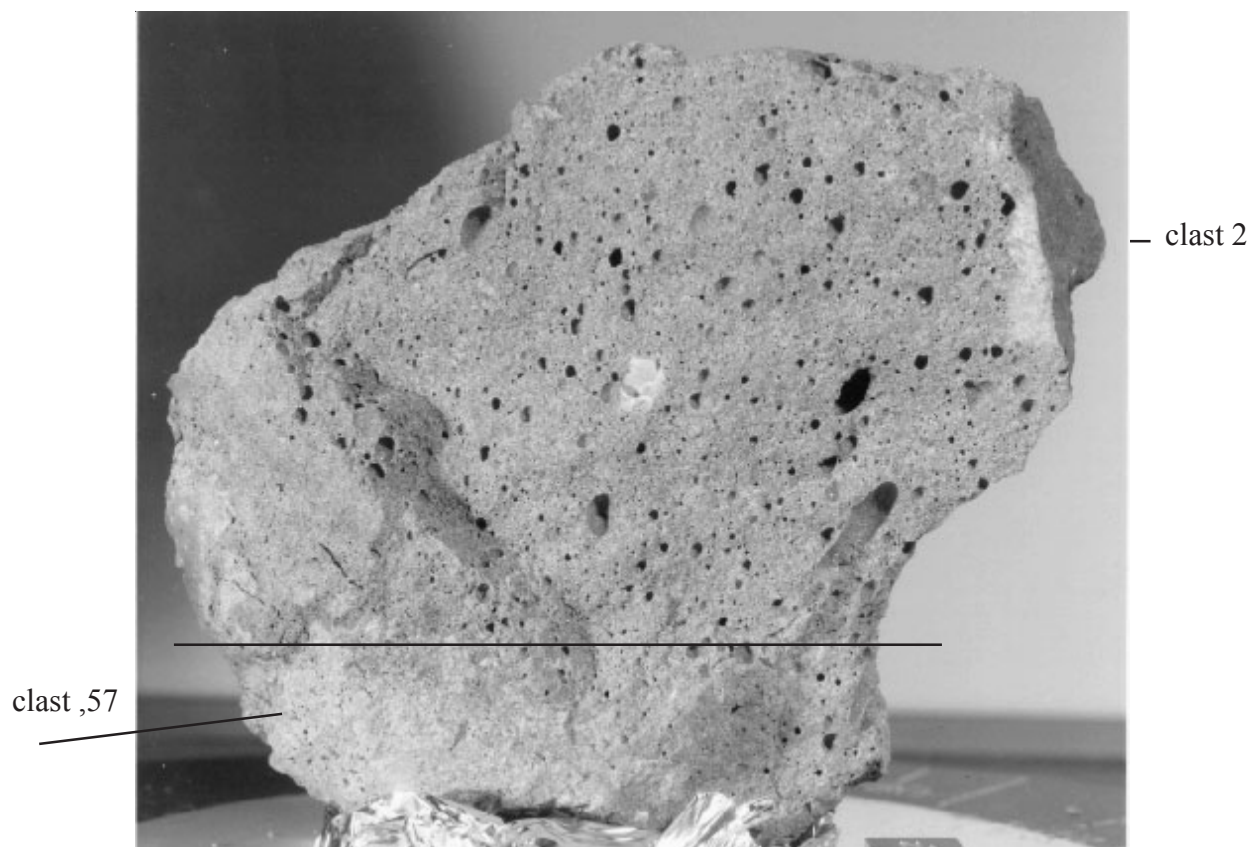


Figure 1: Photo of freshly broken surface of 77135 illustrating clasts and vesicular interior. Edge of cube is 1 cm. Approximate location of saw cut is shown. NASA# S72-56391

### **Introduction**

Sample 77135 was sampled as “green-gray breccia” from the boulder at Station 7. It is an impact melt breccia remarkably similar in textural appearance and chemical composition to 76015 and other samples from the large boulder at Station 6 (Chao et al 1975 and Winzer et al. 1975). The probable origin of impact melt breccias has been explained by Simonds (1975) and Onorato et al (1976). However, some researchers indicate an igneous origin (Storey et al. 1974, Basaltic

Volcanism Study). It has even been equated with “low-K Fra Mauro basalt” (Vaniman and Papike 1980).

In fact, sample 77135 is a vesicular, gray, fragment-laden, fine-grained, crystalline matrix breccia (figure 1). It has two parts: a larger, highly vesicular part which includes clasts of recrystallized troctolitic anorthosite and a smaller less vesicular part which includes recrystallized troctolitic breccia (Minkin et al. 1978).

### **Mineralogical Mode of 77135**

	Minkin et al. 1978		Vaniman and Papike 1979	Chao and Minkin 1975
	More vesicular	Less vesicular		
Pyroxene	31 vol. %	17	30	31
Plagioclase	56	62	41	53
Olivine	7.3	17	15	13
Ilmenite	2.3	3.6	1.4	3
K-rich material	2.6	0.3		

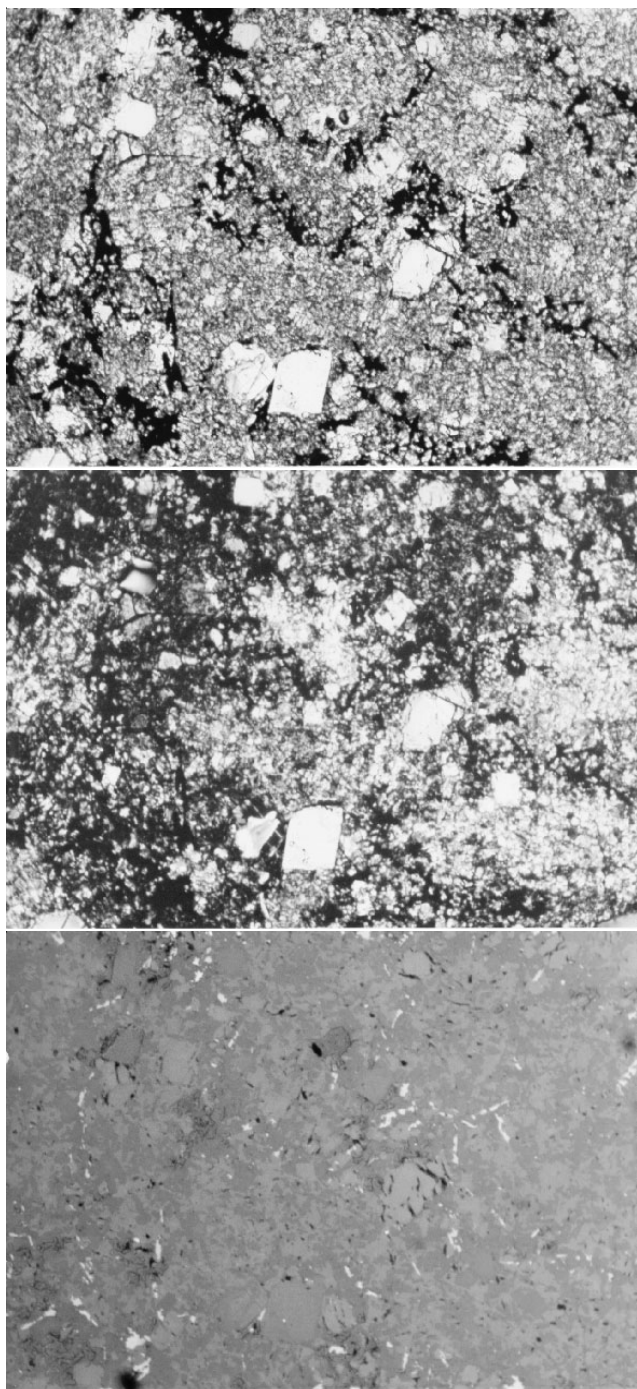


Figure 2: Photomicrographs of thin section 77135,7 illustrating matrix and small clasts. Field of view is 1.4 mm. a) plane polarized light NASA# S79-27747, b) crossed nicols NASA# S79-27748, c) reflected light NASA # S79-27746.

77135 was sampled as the stratigraphically youngest lithology on the Station 7 boulder (Butler and Dealing 1974).

This sample and others from the Station 7 boulder were studied by the International Consortium led by Ed Chao

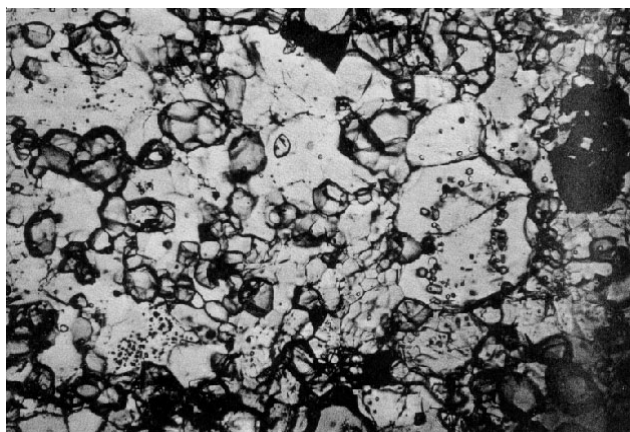


Figure 3: Photomicrograph of small clast in thin section 77135,27. Small polygonal olivine grains in mostly plagioclase matrix (from Chao et al. 1974). This is “anorthositic troctolite” clast 2 (,52).

(see summary by Minkin et al. 1978). The results on 77135 were also summarized in the catalog by Meyer (1994). The crystallization age is about 3.85 b.y. with about 30 m.y. exposure to cosmic rays.

### **Petrography**

Chao et al. (1974), Bence et al. (1974), Chao and Minkin (1975) and McGee et al (1980) have provided descriptions of 77135. It contains two texturally distinct fragment-laden melt rock units: a vesicular, coarser-grained matrix lithology with vesicles 100-500 microns and a less-vesicular, finer-grained matrix lithology with vesicles 50–150 microns. Bence et al. (1974) describe the texture as poikiloblastic, while members of the International Consortium refer to it as “fragment-laden, pigeonite basalt”(Minkin et al. 1978).

The coarse-grained matrix of 77135 consists predominantly of poikilitic pyroxene (mostly pigeonite with minor augite) enclosing subhedral to euhedral plagioclase and minor olivine (figure 2). Borders between pyroxene oikocrysts contain granular olivine, ilmenite plates and rods and mesostasis. The pyroxene oikocrysts enerally are 200-600 microns in size, but some are larger than 1 mm.

The finer-grained matrix commonly surrounds or is adjacent to large lithic clasts. The matrix of the finer fraction also consists predominantly of poikilitic pyroxenes (75-200 microns) enclosing plagioclase. Intergrowths of olivine and plagioclase form aggregates approximately the same size as pyroxene oikocrysts.

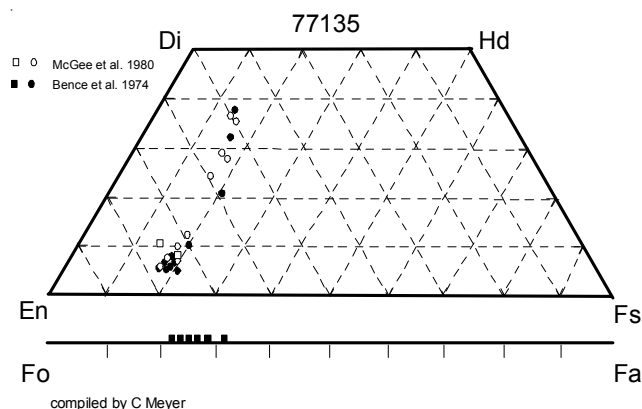


Figure 4: Pyroxene and olivine composition diagram for 77135 (data from McGee et al. 1980, Bence et al. 1974).

There appears to be more olivine, less pyroxene and less vesicles in the finer-grained lithology.

The characteristic poikilitic texture of 77135 and other lunar melt rocks is apparently the result of enhanced growth of pyroxene and ilmenite enclosing smaller grains of feldspar and olivine. Simonds (1973) and Lofgren (1977) explain that poikilitic texture in these melt rocks is the result of two-stage cooling: initial rapid cooling near the coetectic with nucleation of feldspar and olivine at many foci, followed by slower cooling and crystallization at the point where pyroxene saturation is reached, allowing growth of large pyroxene grains encompassing the previous crystals. Ilmenite and other minerals form in the mesostasis between oikocrysts.

### Significant Clasts

Two clasts in 77135 have been carefully extracted (Butler and Dealing 1974), described by Chao et al. (1974) and analyzed by Winzer et al. (1974) and Morgan et al. (1974). The locations of these clasts are shown in figure 1.

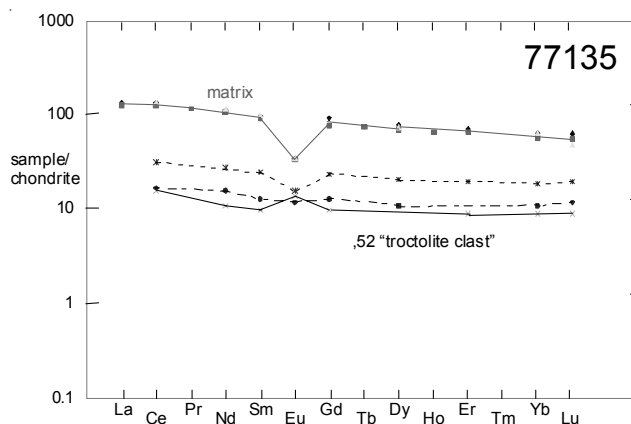


Figure 5: Normalized rare-earth-element diagram for matrix and clasts in 77135 (data from table 1).

### Clast 1 (77135,57) "olivine-rich" clast

According to Chao et al. (1974) the texture of this "recrystallized xenolith" is distinctly metamorphic with many triple-point grain-boundary junctions. The high Ir content (17 ppm) of this clast showed that it was non-pristine (Higuchi and Morgan 1975). Stettler et al. (1978) and Nunes et al. (1974) dated this clast at 3.88 and 3.89 b.y respectively (figures 8 and 10).

### Clast 2 (77135,52) "troctolitic anorthosite" clast

The texture of this clast is metamorphic (figure 3). Morgan et al. (1974) found that this clast had high Ir (non-pristine). Stettler et al. (1974) dated it at 3.99 b.y. (figure 7).

### Mineralogy

**Olivine:** Olivine ( $\text{Fo}_{64-79}$ ) occurs both as rounded inclusions in pigeonite and as irregular grains associated with anhedral plagioclase. Bence et al. (1974), Chao and Minkin (1974), Vaniman and Papike (1980), Smith et al. (1980) and Ryder (1992) analyzed olivine.

### Summary of Age Data for 77135

	Ar39/40	Rb/Sr	
Stettler et al. 1974	3.83 ± 0.04		matrix
	3.99 ± 0.02		clast ,51
Stettler et al. 1975	3.90 ± 0.03		
Stettler et al. 1978	3.88 ± 0.05		clast ,57
	3.87 ± 0.05		clast ,41
Nakamura et al. 1976		4.14 ± 0.08	mixing line ?
Nunes et al. 1974		3.89 ± 0.08	clast ,57
Dalrymple and Ryder 1996	>3.743		

**Caution: Data not corrected for new decay constants.**



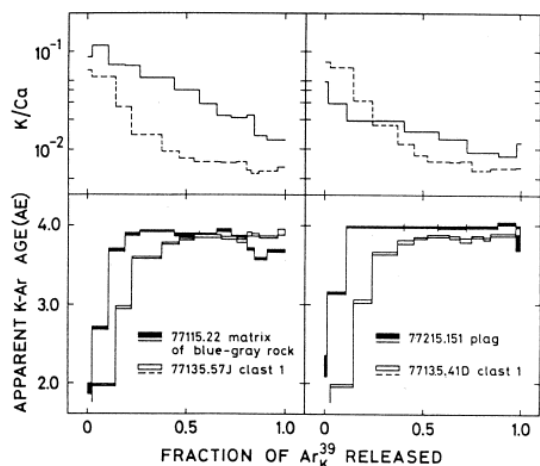


Figure 6: Argon 39/40 release patterns for 77135 clasts .57 and .41 (from Stettler et al. 1978).

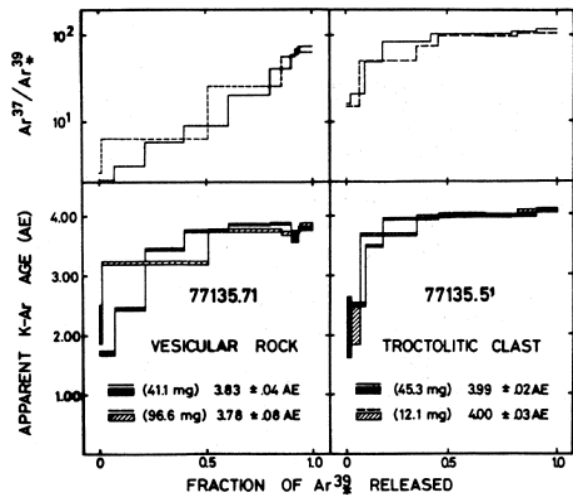


Figure 7: Argon 39/40 release patterns for matrix and clast (.51) in 77135 (from Stettler et al. 1974).

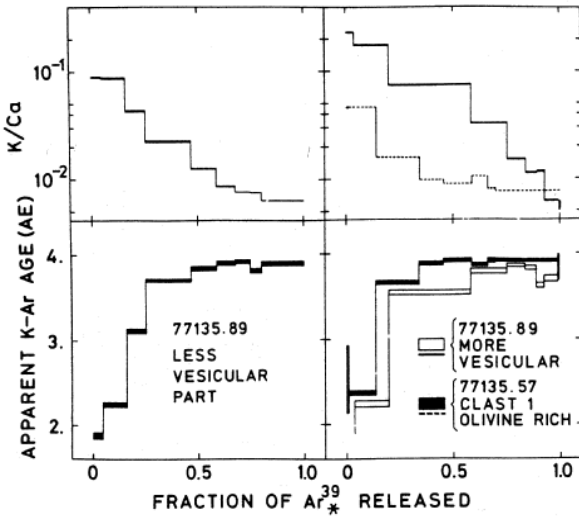


Figure 8: Argon 39/40 release patterns for matrix and clast .57 (from Stettler et al. 1975).

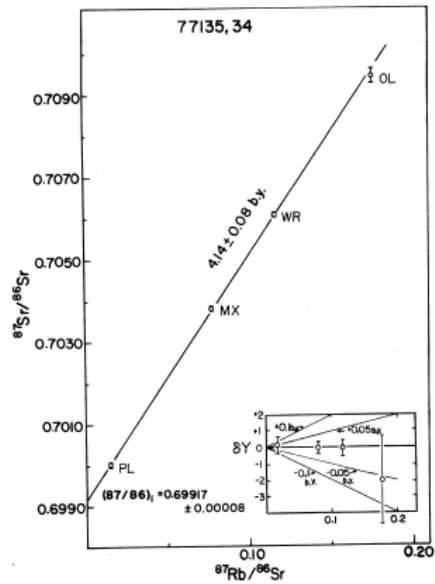


Figure 9: Apparent Rb-Sr mineral "isochron" (or mixing line) for 77135 matrix, including small plagioclase xenoliths. No significance should be given to this "age" (see discussion). Figure from Nakamura et al. (1996).

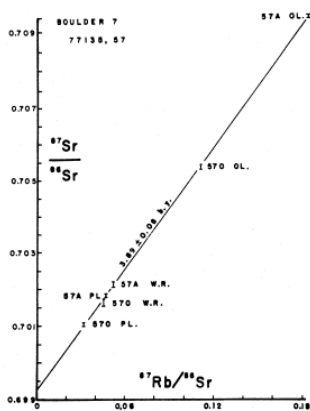


Figure 10: Rb-Sr internal mineral isochron of an olivine-rich clast (.57) in 77135 (from Nunes et al. 1974).

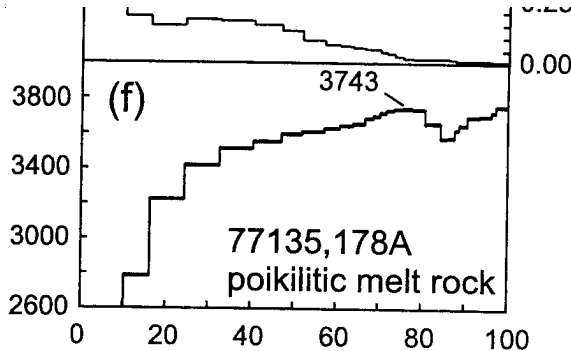


Figure 11: Ar/Ar release pattern for 77135 (Dalrymple and Ryder 1996).

**Table 1a. Chemical composition of 77135.**

reference weight	LSPET 73				Rhodes 74				Norman 02				t. clast Winzer 77				matrix Winzer 74				clast	
	,2				,5								,52 ,82 ,91 ,41				,66 ,77 ,57					
SiO <sub>2</sub> %	46.13	(a)	46.17	(a)	46.1	(b)	44.4	47.5	46.3	45.3	45.3	46.3	(f)									
TiO <sub>2</sub>	1.54	(a)	1.53	(a)	1.48	(b)	0.24	1.45	1.31	0.43	1.72	1.48	(g)									
Al <sub>2</sub> O <sub>3</sub>	18.01	(a)	17.83	(a)	18.5	(b)	27.81	17.18	19.82	25.13	18.03	18.39	(f)									
FeO	9.11	(a)	9.1	(a)	8.04	(b)	4.19	9.01	8.28	5.98	9.56	9.48	(f)									
MnO	0.13	(a)	0.13	(a)	0.12	(b)	0.05	0.11	0.1	0.06	0.11	0.11	(f)									
MgO	12.63	(a)	12.39	(a)	11.6	(b)	7.96	12.66	11.78	8.59	13.38	12.19	(f)									
CaO	11.03	(a)	11.08	(a)	11.1	(b)	15.09	10.91	11.74	13.95	10.64	10.96	(f)									
Na <sub>2</sub> O	0.53	(a)	0.69	(a)	0.71	(b)	0.41	0.66	0.56	0.4	0.61	0.65	(f)									
K <sub>2</sub> O	0.3	(a)	0.27	(a)	0.26	(b)	0.07	0.41	0.21	0.09	0.22	0.23	0.048	(e)								
P <sub>2</sub> O <sub>5</sub>	0.28	(a)	0.3	(a)			0.03	0.29	0.21	0.1	0.28	0.28	(g)									
S %	0.08	(a)	0.07	(a)																		
sum																						
Sc ppm					17.1	(b)																
V					43	(b)																
Cr	1368	(a)			1332	(b)																
Co					17.4	(b)																
Ni	110	(a)	62	(a)	127	(b)																
Cu					18.6	(b)																
Zn	10	(a)	4	(a)	14.6	(b)																
Ga					5.3	(b)																
Ge ppb																						
As																						
Se																						
Rb	7.32	(e)	6.2	(a)	7.2	(b)	2			2.67	5.99	6.63	1.18	(e)								
Sr	172	(e)	174	(a)	194	(b)	147	177	171	147	169	181	87.4	(e)								
Y	107	(a)	111	(a)	117	(b)																
Zr	494	(a)	508	(a)	520	(b)	62.1			146	308	643	71.8	(e)								
Nb	33	(a)	33	(a)	36.1	(b)																
Mo																						
Ru					2.82	(c )																
Rh																						
Pd ppb					3.97	(c )																
Ag ppb																						
Cd ppb																						
In ppb																						
Sn ppb																						
Sb ppb																						
Te ppb																						
Cs ppm					0.28	(b)																
Ba	337	(e)			339	(b)	63.3	360	294	96.6	343	359	60.8	(e)								
La	32.1	(e)			30.1	(b)																
Ce	81.2	(e)			76	(b)	9.63	82.8	59.2	19.4	81.2	83.3	10.5	(e)								
Pr					10.6	(b)																
Nd	51.6	(e)			48.9	(b)	4.99	53.2	41.1	12.7	52.2	54.6	7.14	(e)								
Sm	14.6	(e)			13.9	(b)	1.41	14.8	11.2	3.62	14.7	15.4	1.96	(e)								
Eu	1.99	(e)			1.95	(b)	0.8	1.97	1.8	0.919	2.02	2.16	0.687	(e)								
Gd	18.5	(e)			15.4	(b)	2.03			4.73	18.6	18.6	2.51	(e)								
Tb					2.72	(b)																
Dy	19.1	(e)			17.2	(b)		18.3	15.1	5.07	19.3	20	2.69	(e)								
Ho					3.71	(b)																
Er	11.4	(e)			10.6	(b)	1.5	1.4	8.16	3.24	11.4	11.6		(e)								
Tm																						
Yb	10.5	(e)			9.51	(b)	1.45	10.6	8.11	3.08		10.6	1.79	(e)								
Lu	1.55	(e)			1.37	(b)	0.223	1.18	1.17	0.481	1.56	1.75	0.293	(e)								
Hf					10.5	(b)																
Ta					1.51	(b)																
W ppb					0.64	(b)																
Re ppb					0.17	(c )																
Os ppb																						
Ir ppb					1.37	(c )																
Pt ppb					2.17	(b)																
Au ppb																						
Th ppm	5.6	(e)			5.69	(b)																
U ppm	1.5	(e)			1.47	(b)																

technique (a) XRF (b) ICP-MS, (c ) ICP-ID- MS, (d) RNAA, (e) IDMS, (f) AA, (g) Colorimetric, (h) counting

**Table 1b. Chemical composition of 77135.**

reference	Morgan 74				Higuchi 75	Rancitelli 74	Dalrymple96	
weight								
SiO2 %								
TiO2								
Al2O3								
FeO							8.7	(i)
MnO								
MgO								
CaO								
Na2O							0.67	
K2O					0.22	(e)	0.26	
P2O5								
S %								
sum								
Sc ppm							16.7	(i)
V								
Cr							1359	(i)
Co							16	(i)
Ni	205	174	412	438	221	(d)	122	(i)
Cu								
Zn	2.9	2.6	2.4	3.3	2	(d)		
Ga								
Ge ppb	295	50	78	618	113	(d)		
As								
Se	137	11.3	33	144	40	(d)		
Rb	6.5	1.8	2.6	6.1	3.59	(d)	8	(i)
Sr							190	(i)
Y								
Zr							350	(i)
Nb								
Mo								
Ru								
Rh								
Pd ppb								
Ag ppb	1.1	0.38	0.58	1.2	0.7	(d)		
Cd ppb	10.5	6.8	3.7	3.5	2.4	(d)		
In ppb								
Sn ppb								
Sb ppb	1.21	0.58	0.47	2.16	0.778	(d)		
Te ppb	3.6	1.32	1.1	8.84	5	(d)		
Cs ppm	0.27	0.07	0.07	0.25	0.0953	(d)	0.29	(i)
Ba							346	(i)
La							33.5	(i)
Ce							89.1	(i)
Pr								
Nd							63	(i)
Sm							15.5	(i)
Eu							1.99	(i)
Gd								
Tb							3.3	(i)
Dy								
Ho								
Er								
Tm								
Yb							11.3	(i)
Lu							1.5	(i)
Hf							12.2	(i)
Ta							1.54	(i)
W ppb								
Re ppb	0.49	0.66	1.42	1.06	1.38	(d)		
Os ppb								
Ir ppb	3.78	7.2	15.1	10.5	17.4	(d)		
Pt ppb								
Au ppb	3.57	1.46	4.74	6.45	3.09	(d)		
Th ppm							5.51	(e)
U ppm	1.39	0.26	0.45	1.38	0.59	(d)	1.42	(e)
technique:	(d) RNAA, (e) IDMS, (i) INAA							

**Table 2: Composition of 77135**

	U ppm	Th ppm	K2O %	Rb ppm	Sr ppm	Nd ppm	Sm ppm	technique
Rancitelli et al. 1974	1.42	5.51						counting
Nunes et al. 1974	1.39	5.224						IDMS
Hubbard et al. 1975	1.5	5.6	0.3	7.32	172	51.6	14.6	IDMS
Nakamura et al. 1976			0.226	6.77	167.5			IDMS
Winzer et al. 1974			0.22	5.99	169	52.2	14.7	IDMS
			0.23	6.63	181	54.6	15.4	IDMS
Norman et al. 2002	1.47	5.69		7.2	194	48.9	13.9	ICP-MS

**Pyroxene:** The dominant pyroxene in the matrix of 77135 is pigeonite ( $\text{Wo}_{5-12}\text{En}_{67-76}\text{Fs}_{19-21}$ ). Augite is minor (figure 4). McGee et al. (1980) studied the fine exsolution in pyroxenes in 77135 and other samples of the Station 7 boulder.

**Plagioclase:** Plagioclase in the matrix occurs in two distinct morphological types: as small, sharply-defined laths or elongated platy inclusions ( $\text{An}_{91}$ ) in the poikilitic pyroxene. Vaniman and Papike (1980) give plagioclase analyses ( $\text{An}_{83-97}$ ). Steele et al. (1980) analyzed plagioclase by ion microprobe.

**Ilmenite:** Engelhart (1979) has studied ilmenite in 77135.

### **Chemistry**

Norman et al. (2002) give a complete analysis of the matrix of 77135 (table 1a), which is entirely consistent with that of earlier analyses by Winzer et al. (1974 and 1977), Hubbard et al. (1974) and Rhodes et al. (1974) (figure 5). Morgan et al. (1974) and Hugiuchi and Morgan (1975) have measured the trace element contents of matrix and clasts. Gibson and Moore (1974 and Gibson et al. (1987) give sulfur and hydrogen contents.

### **Radiogenic age dating**

Turner and Cadogan (1975) and Dalrymple and Ryder (1996) found that 77135 gave very poor Ar release patterns, preventing accurate age determination. Apparently there has been a young event that has disturbed isotopic system. Stettler et al. (1974, 1975 and 1978) were able to date the matrix and clasts of 77135 by Ar 39/40 release patterns (figures 6, 7 and 8). Nunes et al. (1974) dated clast 1 by Rb-Sr (figure 10), but Nakamura et al. (1976) were unable to date the matrix due to included clasts. Nunes et al. (1974) reported U-Th-Pb data for 77135.

### **Cosmogenic isotopes and exposure ages**

Rancitelli et al. (1994) measured the cosmic-ray-induced activity as  $^{22}\text{Na} = 100 \text{ dpm/kg.}$ ,  $^{26}\text{Al} = 111 \text{ dpm/kg.}$ ,  $^{46}\text{Sc} = 7.2 \text{ dmp/kg.}$ ,  $^{54}\text{Mn} = 21 \text{ dpm/kg.}$ ,  $^{56}\text{Co} = 66 \text{ dpm/kg.}$  and  $^{60}\text{Co} = 3.4 \text{ dpm/kg.}$

Turner and Cadogan (1975) reported an exposure age of 23 m.y., Stettler et al. (1974 and 1977) determined ages of 28.6 and 29.6 m.y. by  $^{37}\text{Ar}$ . Crozaz et al. (1974) and Eberhardt et al. (1975) reported  $^{81}\text{Kr}$  exposure ages of  $28 \pm 3$  and 31.8 m.y. respectively. Eugster et al. (1984) also discussed the exposure age of 77135.

### **Other Studies**

Fechtig et al. (1974) studied the microcraters on the surface of 77135. Adams and Charette (1975) determined the spectral reflectance. Brecher (1975) measured the Mossbauer spectra. Crozaz et al. (1974) reported a “track age” of  $5.4 \pm 0.8 \text{ m.y.}$

The magnetic properties of 77135 have been studied by Cisowski et al. (1983), Nagata (1975), Pierce et al. (1974), Brecher (1975, 1977) and Hale et al. (1978).

77135 was used to study the residual effect of the 1972 solar flare (Rancitelli et al. 1974, Yokoyama et al. 1974).

Storey et al. (1974) and Ford (1976) have studied 77135 experimentally (it could not have been a liquid below about 1280 deg. C).

### **Processing**

The initial processing and distribution of 77135 is outlined in Butler and Dealing (1974). It was studied by the International Consortium led by Ed Chao (Minkin et al. 1978). Detailed description of the splits is given in USGS open-file report 78-511. The largest piece of 77135 in 2004 weighs 234 grams. There are 34 thin sections.

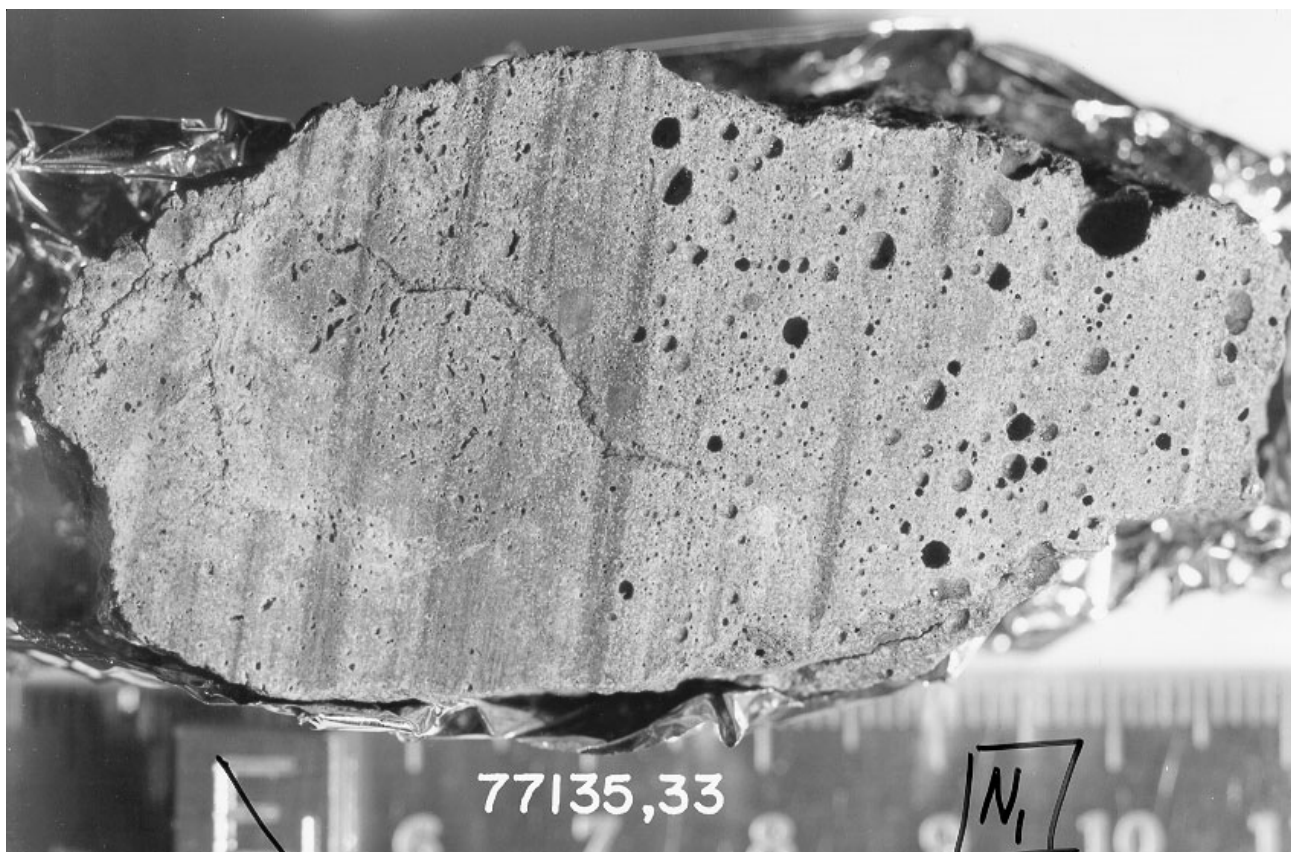
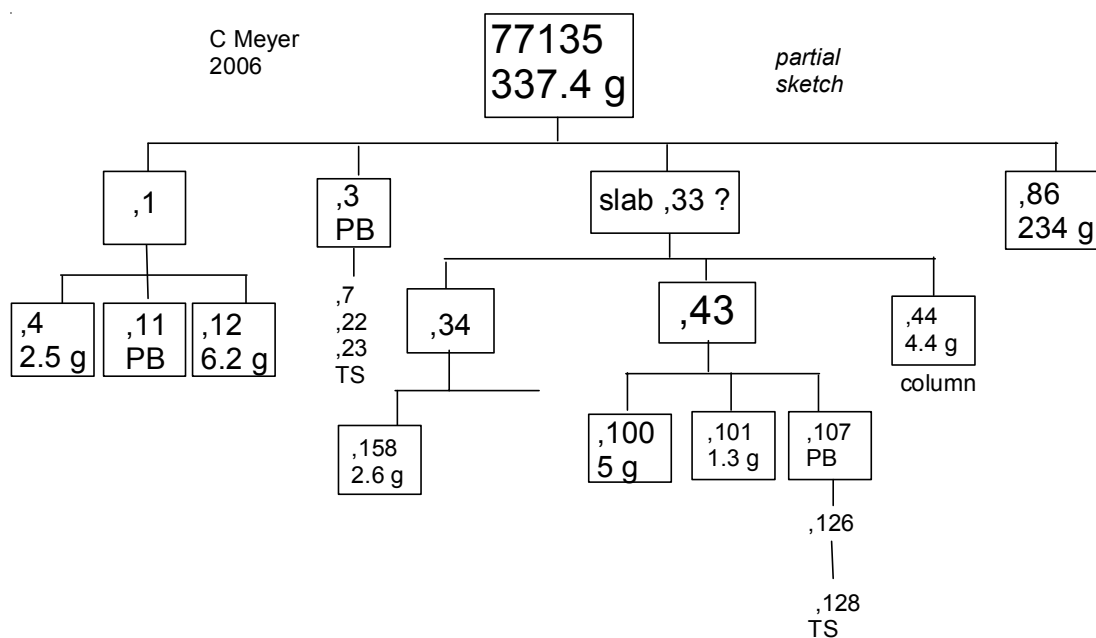


Figure 12: Photo of slab (or end piece) after sawing 77135 showing relic flow banding and vesicularity. NASA S73-34469. Scale in cm.





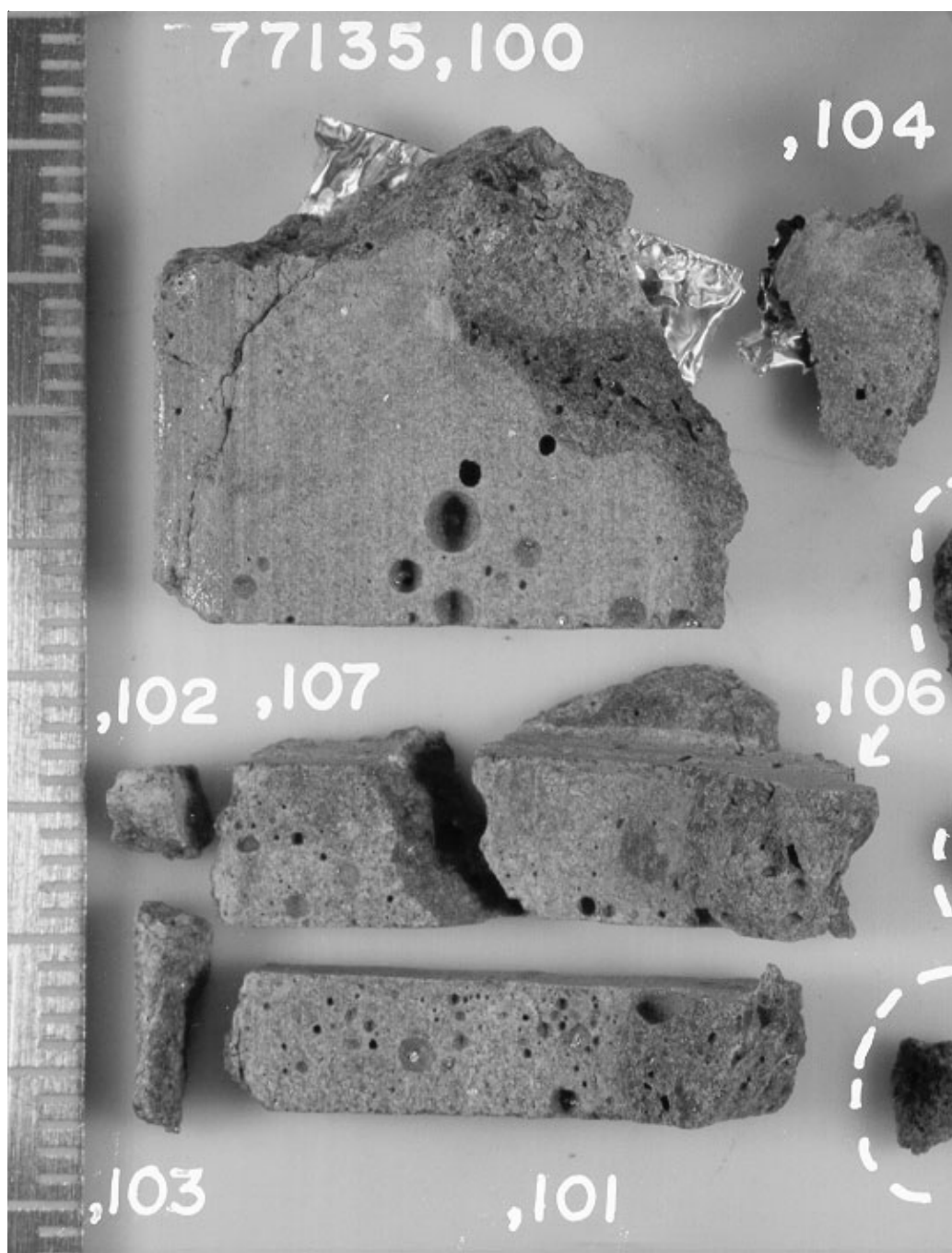


Figure 13: Photo of subdivided slab of 77135,43. NASA S75-21996. Scale is in cm.